

Neutron Scattering Characterization of Pure and Rare-Earth Modified Zirconia Catalysts

James W. Richardson, Jr., Chun-Keung Loong and Pappannan Thiyagarajan

Intense Pulsed Neutron Source Division

Argonne National Laboratory

Argonne, IL 60439 USA

and

Masakuni Ozawa and Sugura Suzuki

Nagoya Institute of Technology

Tajimi, Gifu, 507, Japan

RECEIVED

JUL 26 1999

OSTI

The submitted manuscript has been authored by a contractor of the U. S. Government under contract W-31-109-ENG-38. Accordingly, the U. S. Government retains a nonexclusive, royalty-free license to publish or reproduce the published form of this contribution, or allow others to do so, for U. S. Government purposes.

To be published in Proceedings of the 46th Annual Denver
X-ray Conference:

“Avances in X-ray Analysis”

Plenum Press

*Work supported by U. S. Department of Energy, BES, contract No. W-31-109-ENG-38

DISCLAIMER

This report was prepared as an account of work sponsored by an agency of the United States Government. Neither the United States Government nor any agency thereof, nor any of their employees, make any warranty, express or implied, or assumes any legal liability or responsibility for the accuracy, completeness, or usefulness of any information, apparatus, product, or process disclosed, or represents that its use would not infringe privately owned rights. Reference herein to any specific commercial product, process, or service by trade name, trademark, manufacturer, or otherwise does not necessarily constitute or imply its endorsement, recommendation, or favoring by the United States Government or any agency thereof. The views and opinions of authors expressed herein do not necessarily state or reflect those of the United States Government or any agency thereof.

DISCLAIMER

Portions of this document may be illegible in electronic image products. Images are produced from the best available original document.

Neutron Scattering Characterization of Pure and Rare-Earth Modified Zirconia Catalysts

James W. Richardson, Jr., Chun-Keung Loong and Pappannan Thiyagarajan
Intense Pulsed Neutron Source Division
Argonne National Laboratory, Argonne, IL 60439 USA

and

Masakuni Ozawa and Sugura Suzuki
Nagoya Institute of Technology, Tajimi, Gifu, 507, Japan

Abstract

The combined application of neutron powder diffraction, small angle neutron scattering and neutron inelastic scattering has led to improved understanding of the crystal phases, defect structure, microstructure and hydroxyl / water dynamics in pure and lanthanide-modified zirconia catalysts. Powder diffraction experiments quantified the degree of stabilization and provided evidence for static, oxygen vacancy-induced atomic displacements in stabilized zirconia. Quantitative assessment of Bragg peak breadths led to measurements of "grain size", representing coherency length of long-range ordered atomic arrangements (crystals). Small angle neutron scattering provided a separate measurement of "grain size", representing the average size of the primary particles in the aggregates, and the evolution of porosity (micro- versus meso-) and surface roughness caused by RE modification and heat treatment. Finally, the dynamics of hydrogen atoms associated with surface hydroxyls and adsorbed water was investigated by neutron inelastic scattering, revealing changes in frequency and band breadth of O-H stretch, H-O-H bend, and librational motion of water molecules.

Introduction

High-surface-area zirconia is one of the most commonly used support materials for noble metal or oxygen sensor electrolytes in automobile exhaust-emission-control systems. Zirconia is capable, for instance, of selective conversion of synthesis gas into branched hydrocarbons (1-4) and is used to remove poisonous gases such as CO and NO_x from automobile exhaust to meet recent emission standards (5-7). The key desirable property for these catalytic applications is the ability of zirconia to maintain large surface area, structural stability and surface acidity/basicity over a large range of temperatures. Whereas the stable room temperature form of pure zirconia is monoclinic, with higher symmetry forms at elevated temperatures, doping with small amounts of rare-earth (RE) elements helps stabilize the high symmetry phases over a wide range of temperatures thereby removing the disruptive phase transformations observed in pure zirconia (8). Depending upon the valency of the dopant RE ions (e.g., Nd³⁺ or Ce⁴⁺ substituting for Zr⁴⁺), ionic charge compensation results in oxygen vacancies, which can act as adsorption sites and/or promote strong interactions between metal catalysts and their zirconia supports. In general, RE impurities modify interfacial energies, diffusion coefficients and crystalline anisotropy in a complex manner. As a result, the porosity, particle-size distribution and resistance to sintering vary depending on the dopant element, the preparation method and processing. Furthermore, for many reactions on ZrO₂, surface hydroxyl groups and adsorbed water molecules play an important role. For instance, the isosynthetic reaction of CO/H₂/H₂O over zirconia is derived from surface hydroxyls and CO adsorbed on ZrO₂. While the favorable physical properties of pure and rare-earth modified zirconia are estab-

lished, a complete understanding of these phenomena requires systematic investigations by many different methods.

X-ray diffraction is well known as an analytical tool for characterizing microstructural properties of technologically important materials. Less-well known are the unique properties of neutron scattering which provide additional insights not available with x-rays. Because neutrons interact very weakly with atoms during scattering, typical penetration depths are much higher than achieved with x-rays (measured in fractions of an inch, rather than microns as with x-rays). Neutron scattering, therefore, acts as a bulk probe of structure and/or dynamics. Furthermore, the scattering properties of any given element depends upon its subtle nuclear interaction properties; not strictly upon its atomic number as with x-rays. As a result, some light elements, such as oxygen and hydrogen, have unusually strong scattering profiles. Strong coherent scattering from oxygen is valuable in Neutron Powder Diffraction (NPD) by amplifying the relative contribution from oxygen, leading to enhanced sensitivity to oxygen ordering (e.g., partial versus full ordering). This also enhances Small Angle Neutron Scattering (SANS), which probes structural inhomogeneities on the length scale 1-100 nm. Oxide-based pore systems, such as high surface area zirconia, show strong contrast between dense and porous regions, leading to great sensitivity to particle and/or pore size. Hydrogen has a strong incoherent cross section, which can be exploited both by SANS and by Inelastic Neutron Scattering (INS). For instance, subtle changes in the surface properties of hydroxylated grains are readily seen, leading to detailed assignment of vibrational modes sensitive to changes in hydroxide composition. Collectively, then, NPD, SANS and INS paint an elegant picture regarding microstructural properties of industrial materials such as zirconia catalysts, providing important insights into the relationships between physical and structural properties.

Presented here are results from neutron scattering studies of pure and modified zirconia, much of which has been published elsewhere (9,10). A NPD study was carried out on pure zirconia to follow progressive grain growth resulting from heat treatments at progressively higher temperatures, ranging from 290°C to 700°C. NPD measurements were also made on a modified zirconia. SANS experiments were performed with *in situ* heating of pure zirconia, again with the intention of following progressive grain growth. INS experiments were carried out on a modified zirconia, with varying degrees of hydration.

Materials Preparation and Data Collection

Pure zirconia powder for these studies was synthesized from hydrolysis of a $ZrOCl_2$ aqueous solution at 100°C for ~90 hrs, with subsequent heating at 290°C in air for 3 hrs. The fresh powder was divided into two batches, one each for NPD and SANS. Rare-earth modified zirconia samples were prepared by a coprecipitation technique described elsewhere (7).

NPD experiments were performed on the General Purpose Powder Diffractometer (GPPD) (11) at the Intense Pulsed Neutron Source (IPNS) at Argonne National Laboratory. Powders (5-10 g) were enclosed in thin-wall vanadium cans, and data collected at fixed scattering angles $2\theta = \pm 148^\circ$ (with d-spacing range 0.5 - 3.0 Å) were used for Rietveld analysis (12,13). SANS experiments were carried out on the Small Angle Diffractometers SAD and SAND at IPNS. Samples were enclosed in Supracil cells (sample thickness 2 mm) and maintained at selected temperatures between ambient and 800°C, and data were collected over the Q range 0.001 to 0.2 Å⁻¹. Details about the small-angle diffractometers are given elsewhere (14). Studies of the dynamics of adsorbed hydrogen species on zirconia, studied with INS, were performed using the High-Resolution Medium-Energy Chopper Spectrometer (HRMECS) at IPNS. For this, powdered samples (~40 g) were placed inside sealed aluminum containers in the shape of a thin slab, and mounted to

the cold plate of a closed cycle helium refrigerator for cooling. Two incident energies, 600 and 50 meV, were used to characterize the energy spectrum from 0 to 550 meV.

Neutron Powder Diffraction (NPD)

Neutron powder diffraction is based upon Bragg scattering, characterized by sharp diffraction peaks due to the periodic nature of crystalline lattices. Rietveld profile refinement (12,13), which has become the standard analysis technique for powder diffraction data, performs least-square refinements of adjustable parameters defining the structures to best fit the entire diffraction pattern. The technique has developed to the point where a multitude of phases (reliably up to 6-8 depending on the complexity of the phases present) can be refined simultaneously, including parameters quantifying interatomic distances and angles, phase fractions, microstrain and coherency length (particle size).

Pure ZrO_2 has three polymorphs: a cubic fluorite structure (space group $Fm\bar{3}m$) above $2367^\circ C$, a tetragonal structure ($P4_2/nmc$) between 1127 and $2367^\circ C$, and a monoclinic structure ($P2_1/c$) below $1127^\circ C$. Modified zirconias typically contain a mixture of cubic and tetragonal (or monoclinic) phases, retained metastably over a wide range of temperatures including room temperature. Rietveld profile refinement of NPD data can quantify structural parameters for all phases present, including atomic positions, site occupancies, lattice parameters and volume fractions, thus providing precise assessment of vacancy concentration and degree of stabilization.

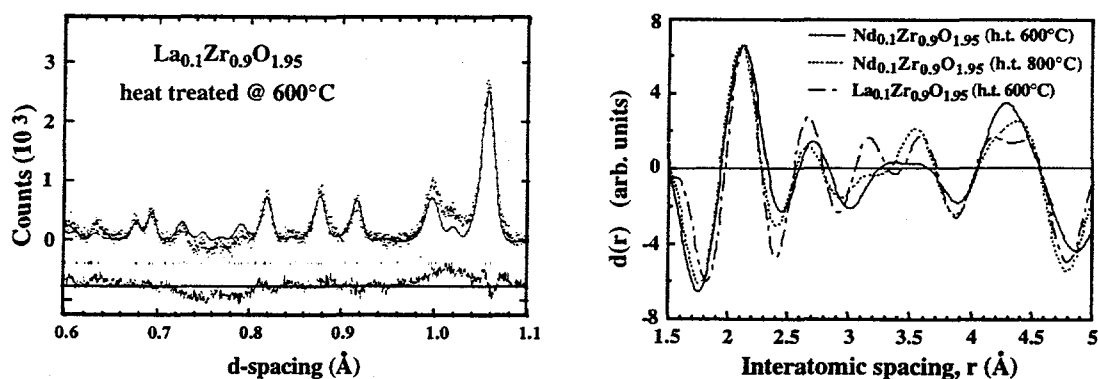


Figure 1. Rietveld profile fit for $Nd_{0.1}Zr_{0.9}O_{1.95}$ powder subjected to heat treatment at $600^\circ C$. Dots are observed intensities, solid line represents calculated crystalline intensities, and tick marks indicate positions of the Bragg reflections in cubic (top row) and tetragonal (bottom row) phases, and tetragonal phases. Residual intensities shown at the bottom show evidence for oscillatory diffuse scattering. Shown in (b) are correlation functions calculated from residual intensities as in (a).

Incoherence among crystalline grains, such as a distribution of grain sizes, grain boundaries and microstrains, causes deviations in observed Bragg-peak intensities from those expected for an ideal powder. Within the Rietveld refinement, some of these effects such as the average grain size and microstrain can be modeled by adjustable parameters (15). Furthermore, short-range atomic disorder such as defects, compositional fluctuations, atomic displacements from lattice sites, give rise to another type of coherent scattering which may be manifest as a diffuse, variant component superimposed on the Bragg scattering. Some features of the short-range order structure may be revealed in terms of a real-space correlation function which can be extracted from a Fourier filtering analysis (16).

Rietveld analysis of a powdered sample of $\text{La}_{0.1}\text{Zr}_{0.9}\text{O}_{1.95}$ (heat-treated at 600°C), assuming random substitution of La for Zr, resulted in identification of the metastable cubic and tetragonal forms of ZrO_2 . Figure 1a shows the observed (with traditional background subtracted), calculated and difference powder patterns from that refinement. While the Bragg peak breadths are reasonably sharp, indicating minimal particle size broadening, an oscillatory component is recognizable in the residual, due to composition fluctuations from oxygen vacancies. Fourier transformation of the residual curve yielded a correlation function, $d(r)$, similar to the radial distribution function used to describe amorphous materials. Shown in Figure 1b are $d(r)$ functions obtained for three Ln- ZrO_2 , with maxima at about 2.105, 2.68, 3.16, 3.47 and 4.35 Å, corresponding to 1st neighbor Zr-O, 1st neighbor (O-O', O-O'' and O-O''') and 1st neighbor Zr-Zr interatomic spacings, respectively. These values are slightly shifted from idealized distances in cubic ZrO_2 , suggesting that the diffuse scattering is from assemblages of atoms displaced from optimal positions, e.g., toward oxygen vacancies.

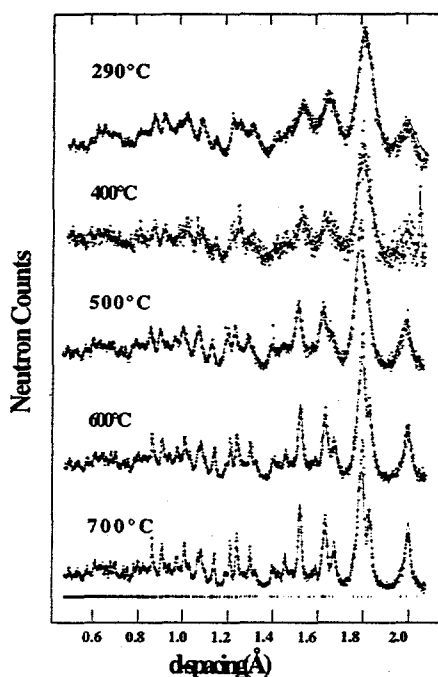


Figure 2. Rietveld profile fits for pure ZrO_2 samples heat-treated at temperatures in the range $290\text{--}700^\circ\text{C}$. Dots and solid lines represent observed and calculated crystalline intensities, respectively. Tick marks at the bottom identify positions of Bragg reflections. Note progressive sharpening of Bragg peaks resulting from grain growth.

NPD Rietveld profile fits for pure zirconia after annealing at 290° (as prepared), 400° , 500° , 600° , and 700°C are shown in Fig. 2. All of the patterns show monoclinic symmetry, as expected for ZrO_2 , and extremely broad peaks. The peaks sharpen progressively with increasing annealing temperature, indicating continuous grain growth and relaxation of internal microstrain. Observed peaks in the sample heat treated at 700°C are still much wider than corresponding ones in a commercial ZrO_2 powder prepared by high-temperature ($>900^\circ\text{C}$) techniques, suggesting that grain growth would continue at higher annealing temperatures. Calculated particle sizes for annealed ZrO_2 are presented in Figure 3, along with values obtained from SANS (see text below).

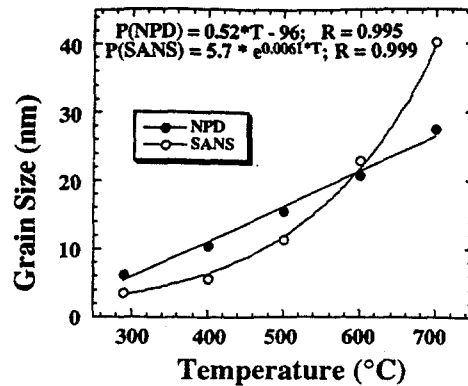


Figure 3. Average particle sizes for pure ZrO_2 from analysis of Bragg peak broadening in NPD and crossover regions in SANS data. Differences in absolute values and behavior with increasing temperature are probably due to differences in the properties probed by the two techniques.

Small Angle Neutron Scattering (SANS)

While conventional powder diffraction yields information regarding the average structure of atomic organization over a length scale of typically a crystalline unit-cell dimension, small-angle scattering provides a characterization of inhomogeneities up to ~ 100 nm. Scattering at low wavevector, $Q = 4\pi\sin\Theta/\lambda$ (where Θ is the scattering angle and λ is the neutron wavelength) arises from fluctuations of neutron-scattering cross section in the sample. In the present case, the scattering contrast comes from the zirconia particles versus the pores.

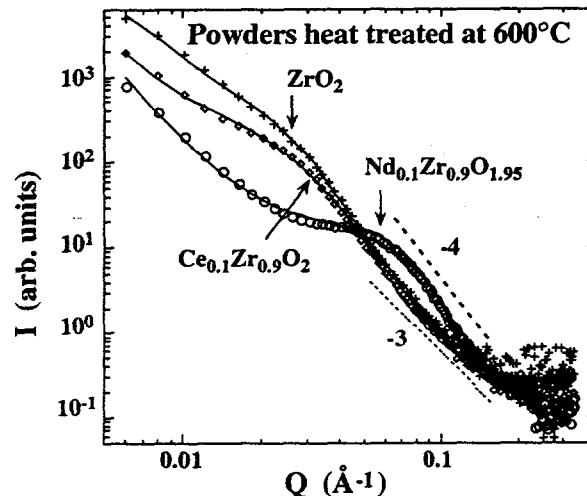


Figure 4. Small angle neutron scattering (SANS) intensities vs. Q for $Nd_{0.1}Zr_{0.9}O_{1.95}$, $Ce_{0.1}Zr_{0.9}O_2$ and ZrO_2 . Solid lines represent fits to the data using a fractal model. Limiting slopes for power-law behavior are given by dotted lines.

Figure 4 shows SANS data in terms of log-intensity versus log- Q profiles taken at ambient temperature for $Nd_{0.1}Zr_{0.9}O_{1.95}$, $Ce_{0.1}Zr_{0.9}O_2$ and ZrO_2 heat-treated at $600^\circ C$. The intensity profiles

of the three samples show distinct Q -dependence, implying RE-dopant specific microstructural changes induced by the modification. In addition, each profile shows a break at a certain Q (denoted by an arrow in Fig. 4) which roughly marks a change of slope in the curve. The position of this breaking point shifts progressively to lower Q for ZrO_2 , $Ce_{0.1}Zr_{0.9}O_2$ and $Nd_{0.1}Zr_{0.9}O_{1.95}$, suggesting a corresponding increase in mean particle size.

The structures of ramified objects formed by aggregates of small particles has been studied extensively by a variety of experimental methods including small-angle scattering (17-19). As in earlier studies (20,21), the scattering function for a mass fractal was used to model the data. By definition the total mass of a mass fractal scales with its radius to its fractal dimension power, i.e., $M \propto r^D$, where D is the fractal dimension. Included in models for the SANS scattering profile are parameters defining the mean particle size and the size distribution. Figure 5 shows the evolution of SANS profiles for pure ZrO_2 subjected to *ex-situ* heat treatments from 290° to 800°C. Again, a progressive change in the particle size and porosity resulting from annealing was observed, and the fractal model describes very well the data of pure ZrO_2 up to the heat-treatment temperature of 500°C (see Fig. 5). As the samples were annealed from 290° to 500°C, the mean particle size increased from ~3.62 nm to ~11.2 nm, and the size distribution expanded from $\sigma = 1.05$ to $\sigma = 1.32$. At higher temperatures, although the fractal model provided a good fit to the data and confirmed the trend of particle coarsening, the fractal dimensions no longer made physical sense, suggesting that the particles had grown in size to an extent that self-affinity behavior could not be sustained over an increasing length scale. Instead, the assembly is better described as a random packing of solid particles with intertwining macroporosity.

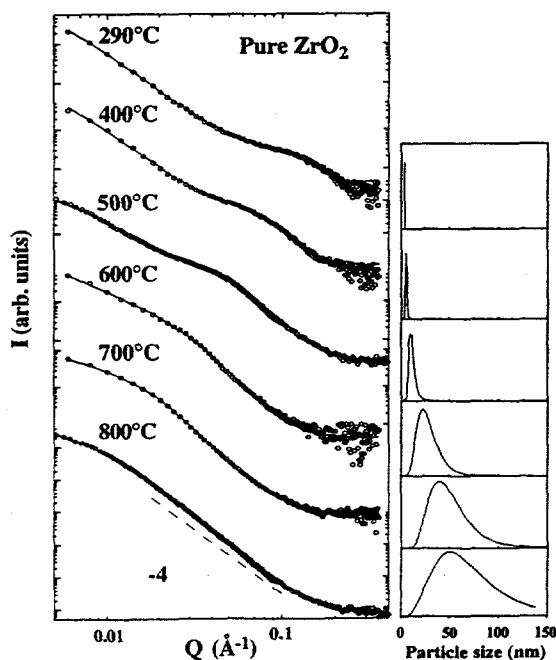


Figure 5. SANS data for pure ZrO_2 . Solid lines for annealing temperatures less than or equal to 500°C are fits to the data using the fractal model, while those for other temperatures are fits used a random packing of hard spheres model. Plots on the right display particle size distributions corresponding to different annealing temperatures.

Inelastic Neutron Scattering (INS)

In our pure ZrO_2 powder, prepared directly from aqueous solution at 100°C , followed by a heat treatment at 290°C , very small (< 10 nm) microcrystallites were initially formed and subsequently grew to somewhat larger size. The micro- and/or mesoporous structure of the powder provides a large effective surface area for the adsorption of hydroxyl groups and water. NPD results (ref. 10, but not presented here) suggest that the surface chemistry, controlled to a large extent by the chemisorbed hydroxyl groups and physisorbed water molecules, are quite sensitive to the underlying crystal structure, defects, and texture parameters. This feature can be seen in the dynamics of the adsorbed hydrogen species in these materials, to be discussed in the next section.

Inelastic scattering measurements were performed on the following high-surface-area samples: "dry" powder, $\text{Nd}_{0.1}\text{Zr}_{0.9}\text{O}_{1.95}$ (heated at 450°C in air for 3 hrs); "low" water content powder, with 0.33 : 44 mass ratio of water : zirconia; a "medium" water content powder, 1.12 : 44 ratio; and a "high" water content powder, 1.8 : 37.6 ratio. Assuming an average of 4.6 H_2O to cover a fully hydroxylated surface of 100 \AA^2 , as found in silica (22), the adsorbed water in the low water content Nd-ZrO_2 and ZrO_2 samples, the medium water content Nd-ZrO_2 , and high water content La-ZrO_2 samples correspond to statistically 0.747, 0.882, 2.54, and 4.46 layers of adsorbed water on the surface, respectively. It should be noted, however, that water adsorption on zirconia surfaces in general does not show distinct steps of layer adsorption. We expect that initially individual water molecules are attached to distinct surface OH groups. As the coverage increases, the tendency of water towards self-association via hydrogen bonding leads to the formation of cluster species prior to the completion of a monolayer coverage. These results were found sensible in the context of earlier Fourier Transform Infrared Spectroscopy (FTIR) studies (23-25).

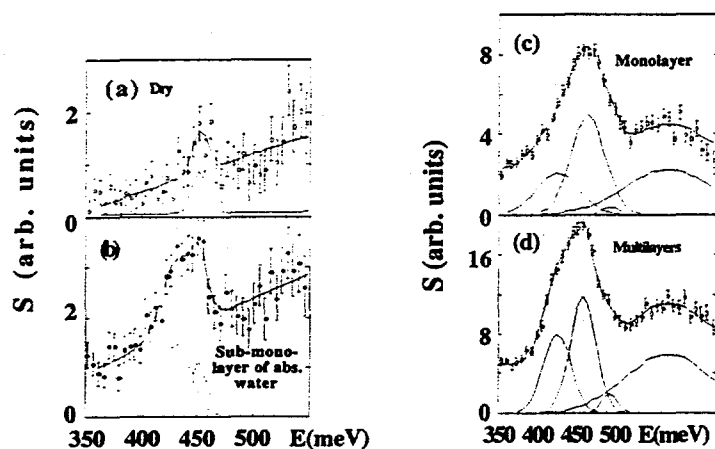


Figure 6. O-H stretch vibration band and combination band fitted to a sum of multiple Gaussian functions and a background for the dry (a), low water content (b), medium water content (c), and high water content (d) samples of lanthanide modified zirconia.

Figure 6 shows an overview of the observed scattering functions for all the samples, taken with an incident neutron energy of 600 meV at 15 K. For the dry samples, containing only chemisorbed surface OH groups, there are broad features in the 400-500, ~ 200 , and < 150 meV regions. The hydrogen vibrational density of dry ZrO_2 is significantly higher than that of dry Nd-ZrO_2 . This reflects the fact that the larger surface area of pure monoclinic ZrO_2 accommodates a substantial increase of OH adsorption. As the coverage of water increases, four bands develop: a librational band at ~ 80 meV due to intermolecular vibrations of the H_2O molecules, two intramolecular

bands, one at ~200 meV due to H-O-H bending and the other at ~430 meV due to O-H stretch, and a combination band at ~506 meV. The low-energy spectra obtained from the 50 meV runs (not shown) exhibit the growth of a peak at ~8 meV with increasing water coverage.

Conclusions

Trends in the estimated particle size as a function of annealing temperature, calculated from Neutron Powder Diffraction (NPD) and Small Angle Neutron Scattering (SANS), are in general agreement. Difference can be attributed to the fact that the different experimental techniques probe different aspects of the microstructure and the resulting parameters need not be identical. For example, the crystalline grain size obtained from NPD represents the coherency of atomic long-range order of a global crystal structure, whereas the particle size obtained from SANS represents the average size of the primary particles in the aggregate. Below the annealing temperature of 600°C the crystalline grains are larger than the primary particles which were nucleated from the hydrolyzed solution. Our NPD results suggest the presence of orientational coherency among the crystalline primary particles. As annealing temperature increases up to about 500°C, microporosity evolves to mesoporosity as particles grow in size and in size distribution. Above 500°C a more abrupt change of the microstructure occurs which leads to a crossover from a mass-fractal-like aggregate to a random packing of solid particles featuring reduced surface area and macroporosity.

Hydrogen densities of states of absorbed OH groups and water on Ln-ZrO₂ and in pure ZrO₂ were measured over an energy range of 0 to 550 meV (0-4440 cm⁻¹). Vibration frequencies characteristic of O-H stretch vibrations as well as inter- and intramolecular vibrations of H₂O were monitored from submonolayer coverage to sapillary condensation of water.

Acknowledgments

Work performed at Argonne National Laboratory is supported by the US DOE, Basic Sciences under Contract No. W-31-109-ENG-38.

References

1. Y. Nakano, T. Iizuka, H. Hattori and K. Tanabe, *J. Catal.* **57**, 1 (1979).
2. S. C. Tseng, N. B. Jackson, and J. G. Ekerdt, *J. Catal.* **109**, 284 (1988).
3. R. G. Silver, C. J. Hou and J. G. Ekerdt, *J. Catal.* **118**, 400 (1989).
4. H. Kuno, K. Takahashi, M. Shibagaki, K. Shimazaki and H. Matsushita, *Bull. Chem. Soc. Jpn.* **63**, 1943 (1990).
5. M. Ozawa and M. Kimura, *J. Less-Common Metals* **171**, 195 (1991).
6. S. Matsumoto, N. Miyoshi, T. Kanazawa, M. Kimura, and M. Ozawa, in "Catalytic Science and Technology" (S. Yoshida, N. Takezawa, and T. Ono, Eds.), Vol. 1, p. 335, Kodansha Ltd., Tokyo, 1991.
7. M. Ozawa, M. Kimura, A. and Isogai, *J. Alloys Compounds* **193**, 73 (1993); and United States Patent No. 5,075,276 (1991).
8. D. J. Green, R. H. J. Hannink and M. V. Swain, "Transformation toughening of ceramics" ed. CRC Press, Boca Raton, FL, 1989.
9. C.-K. Loong, J. W. Richardson, Jr. and M. Ozawa, *J. Catal.* **157**, 636 (1995).
10. C.-K. Loong, P. Thiyagarajan, J. W. Richardson, Jr., M. Ozawa and S. Suzuki, *J. Catal.*, in press (1997).

11. J. D. Jorgensen, J. Faber, Jr., J. M. Carpenter, R. K. Crawford, J. R. Hauman, R. L. Hitterman, R. Kleb, G. E. Ostrowski, F. J. Rotella and T. G. Worlton, *J. Appl. Cryst.* **21**, 321 (1989).
12. H. M. Rietveld, *J. Appl. Cryst.* **2**, 65 (1969).
13. A. C. Larson and R. B. Von Dreele (1986) GSAS, General Structure Analysis System. Los Alamos National Laboratory Report LAUR86-748.
14. P. Thiyagarajan, J. E. Epperson, R. K. Crawford, J. M. Carpenter, T. E. Klippert and D. G. Wozniak, *J. Appl. Cryst.* **30**, in press (1997).
15. H. P. Klug and L. E. Alexander, "X-ray diffraction procedures for polycrystalline and amorphous materials", second ed. John Wiley & Sons, New York (1974).
16. J. W. Richardson, Jr. and J. Faber, Jr., *Adv. X-ray Analysis* **29**, 143 (1985).
17. T. Freltoft, J. K. Kjems and S. K. Sinha, *Phys. Rev.* **B33**, 269 (1986).
18. S. K. Sinha, *Physica* **D38**, 269 (1989).
19. F. Rubio, J. Rubio and J. L. Oteo, *J. Mat. Sci.* **16**, 49 (1997).
20. S. K. Sinha, T. Freltoft and J., in "Kinetics of aggregation and gelation.", (F. Family and D. P. Landau, p. 87. Elsevier Science Publishers B. V., Amsterdam (1984).
21. J. Teixeira, in "On Growth and Form, Fractal and non-fractal patterns in physics.", (H. E. Stanley and N. Ostrowsky, p. 145. Martinus Nijhoff Publishers, Dordrecht (1986).
22. E. W. Kaler, in "Modern aspects of small-angle scattering.", (H. Brumberger, p. 329. Kluwer Academic Publishers, Dordrecht, The Netherlands (1993).
23. J. Erkelens, H. Th. Rijnten and S. H. Eggink-du Burck, *Recueil* **91**, 1426 (1972).
24. P. A. Agron, E. L. Fuller, Jr. and H. F. Holms, *J. Colloid Interface Sci.* **52**, 2482 (1978).
25. W. Hertl, *Langmuir* **5**, 96 (1989).